Farnesyltransferase Inhibitor, ABT-100, Is a Potent Liver Cancer Chemopreventive Agent

Vinicio Carloni, Francesco Vizzutti, and Pietro Pantaleo

Abstract

Purpose: Treatment of hepatocellular carcinoma raised on cirrhotic liver represents a major endeavor because surgery and chemotherapeutic management fail to improve the clinical course of the disease. Chemoprevention could represent an important means to inhibit the process of hepatocarcinogenesis. Farnesyltransferase inhibitors are a class of drugs blocking the growth of tumor cells with minimal toxicity towards normal cells.

Experimental Design: In the present study, we investigated the effects of a novel farnesyltransferase inhibitor, ABT-100, on human liver cancer cell lines, HepG2 and Huh7, and on an animal model of hepatocarcinogenesis.

Results: ABT-100 inhibited HepG2 and Huh7 cell growth as well as the invading ability of Huh7 on Matrigel. In HepG2 and Huh7 cells, ABT-100 inhibited growth factor–stimulated phosphoinositide 3-kinase and Akt/protein kinase B activity. Furthermore, ABT-100 inhibited Akt-dependent $p27^{Kip1}$ phosphorylation and this event was associated with increased levels of $p27^{Kip1}$ in the nucleus and reduced activity of the cyclin-dependent kinase 2. Moreover, ABT-100 treatment resulted in a significant reduction in tumor incidence and multiplicity.

Conclusions: Taken together, these findings identify a mechanism of ABT-100 function and show the efficacy of ABT-100 as a chemopreventive agent of hepatocellular carcinoma.

Hepatocellular carcinoma is one of the most frequent cancers in the world. Currently, survival remains poor for most patients with hepatocellular carcinoma, which is due to the aggressiveness of the lesions at the time of diagnosis and the lack of an effective therapy (1).

With regard to risk factors, several studies have clearly shown that viruses, chemicals, hormones, and metabolic diseases all play an important role in the pathogenesis of the disease. Among these risk factors, however, liver cirrhosis plays a major role. Cirrhosis is characterized by wide fibrosis with presence of nodules containing proliferating hepatocytes. Most of the time continuous and irregular proliferation associated with inflammation may produce genetic cellular abnormalities with development of hepatocellular carcinoma (2–4). This mechanism is responsible for the common association between cancer and cirrhosis. Therefore, studies aimed at hepatocellular carcinoma prevention should consider cirrhosis as a precancerous condition. Another important point to underline is that surgery and chemotherapeutic management of hepatocellular carcinoma fail to improve the clinical course of the disease. Therefore, chemoprevention programs are crucial to decrease the mortality rate for primary liver cancer. Cancer chemoprevention has emerged as an important means of modulating the process of carcinogenesis (5).

Farnesyltransferase inhibitors are a new class of drugs which block the growth of tumors with minimal toxicity in normal cells (6). These compounds inhibit protein farnesyltransferase, an enzyme that catalyzes the farnesylation of a number of proteins including the small GTP-binding protein Ras. Ras is a key regulator of cell growth in all eukaryotic cells. Genetic and biochemical studies have shown the central role played by Ras in signal transduction pathways that respond to diverse extracellular stimuli, including growth factors, cytokines, and extracellular matrix proteins. Previous studies have shown that inhibition of Ras farnesylation blocks Ras-mediated cellular transformation (7–10).

Several studies have confirmed the important role of phosphoinositide-3-kinase (PI3K) in the process of cell transformation mediated by Ras. In fact, dominant-negative p85, a regulatory subunit of PI3K, strongly inhibits transformation by mutant Ras V12. Moreover, active PI3K is sufficient to transform cells. Akt/protein kinase B (PKB), a family of serine-threonine protein kinases has been identified as a direct target of PI3K (11). Akt controls key cellular processes such as cell cycle progression and apoptosis and activated Akt can contribute to tumorigenesis *in vivo*. Phosphorylation of Thr^{308} and Ser^{473} in the COOH-terminal domain is required for full activation of Akt. In human cancer, constitutive activation of PI3K and its effector Akt arise through oncogenic receptor tyrosine kinase, Ras activation and mutational loss of PTEN (12, 13). Akt can increase cyclin D1 levels and down-regulate mitotic inhibitor $p27^{Kip1}$ by increasing $p27^{Kip1}$ proteolysis or

Authors' Affiliation: Dipartimento di Medicina Interna, Università di Firenze, Florence, Italy

Received 11/23/04; revised 2/14/05; accepted 3/9/05.

Grant support: Supported in part by Ministero Italiano dell'Università e della Ricerca Scientifica e Tecnologica (PRIN 2004).

The costs of publication of this article were defrayed in part by the payment of page charges. This article must therefore be hereby marked *advertisement* in accordance with 18 U.S.C. Section 1734 solely to indicate this fact.

Requests for reprints: Vinicio Carloni, Dipartimento di Medicina Interna, Università di Firenze, Viale Morgagni 85, I-50134 Florence, Italy. Phone: 39-55-4296487; Fax: 39-55-417123; E-mail: v.carloni@dmi.unifi.it.

repressing $p27^{Kip1}$ expression through Akt phosphorylation of forkhead transcription factor (14). The progression of human hepatocellular carcinoma has been related with various cell cycle regulators. It has recently been reported that $p27^{Kip1}$ expression could be an independent prognostic marker for disease-free survival in hepatocellular carcinoma. Commonly, hepatocytes do not express $p27^{Kip1}$, however, hepatocellular carcinoma may contain elevated concentration of $p27^{Kip1}$ protein suggesting that other mechanisms are activated inside the cells to block $p27^{Kip1}$ growth inhibition. Because the growth-inhibiting activity of $p27^{Kip1}$ depends on its nuclear localization, the altered compartmentalization of $p27^{Kip1}$ could impair function, and its phosphorylation represents a limiting step in regulating $p27^{Kip1}$ localization (15).

Here we show that ABT-100, a potent farnesyltransferase inhibitor, reduces hepatocellular carcinoma cell growth and diethylnitrosamine-induced hepatocarcinogenesis. Furthermore, in this study, we show that ABT-100-dependent inhibition of PI3K-Akt-induced $p27^{Kip1}$ phosphorylation was associated with an increased nuclear level of $p27^{Kip1}$ protein. Consequent to the accumulation of $p27^{Kip1}$ on PI3K-Akt blockade, $p27^{Kip1}$ was associated with nuclear cyclin-dependent kinase 2 (CDK2) and inhibited CDK2 kinase activity.

Materials and Methods

Drug preparation. The ABT-100 (*S*)-6-[2-(4-cyanophenyl)-2-hydroxy-2-(1-methyl-1H-imidazol-5-yl)ethoxy]-4′-(trifluoromethoxy)-1,1′-biphenyl-3-carbonitrile was provided by Abbott Laboratories (Abbott Park, IL). For *in vitro* studies, ABT-100 was dissolved in DMSO with dilutions made using DMEM plus 10% fetal bovine serum (FBS). The compound was dissolved using 2% ethanol, 8% Solutol HS 15 (BASF, Germany) and 90% hydroxypropylmethylcellulose for *in vivo* studies. This vehicle was used for all s.c. injections.

Antibodies and reagents. The affinity-purified polyclonal antibody to Akt1/PKBα and $p27^{Kip1}$ were purchased from Upstate Biotechnology (Lake Placid, NY). Mouse monoclonal antibodies anti-pY, anti-histone H1 (AE-4) and polyclonal antibodies to CDK2, Rap1A and His-tag $p27^{Kip1}$ were acquired from Santa Cruz Biotechnology (Santa Cruz, CA). Mouse monoclonal antibody to Ras was from Transduction Laboratories (Lexington, KY). Histone H2B and histone H1 were from Roche Biochemicals (Germany).

Cell lines. The following cell lines were used: HepG2 cells derived from a human hepatoblastoma expressing wild-type p53 and Huh7 cells derived from a hepatocellular carcinoma expressing high levels of mutated p53 (point mutation at codon 220). The cells were maintained in DMEM (Sigma Chemical, Co., St. Louis, MO) and supplemented with 10% FBS, 5 mmol/L sodium pyruvate, and 5 mmol/L nonessential amino acids at 37°C in a humidified incubator containing 5% CO_2.

Cell growth and soft agar assay. Cell growth inhibition assay was done by plating 2×10^4 cells on 12-well plates, in DMEM with 10% FBS. Cells were counted after 48 hours' incubation with increasing concentrations of ABT-100 in DMEM with 10% FBS or treated with ABT-100 (20 μmol/L) or DMSO every 48 hours for 6 days. The number of cells was determined at each time point by counting with a hemocytometer every 2 days. Cell viability was measured by trypan blue dye exclusion.

Soft agar assay was done on Huh7 cells. Huh7 were seeded at a density of 1×10^4 cells per well in a 0.3% top agarose layer in DMEM supplemented with 10% FBS over a bottom agarose layer (0.8%). The top layer contained 0.1% DMSO or the indicated concentration of ABT-100 in 0.1% DMSO. The number of colonies per well (aggregates >50 μmol/L) were revealed using a phase contrast microscope 14 days after the cultures were seeded.

Invasion assay. Huh7 cells that show a great ability to invade Matrigel were plated in 100 mm Petri dishes and treated with ABT-100 or DMSO. Cell invasion assay was done using a Boyden chamber equipped with 8 μm porosity polyvinylpyrrolidone-free polycarbonate filter. Polycarbonate filters were coated on the upper surface with 10 μg of Matrigel (Collaborative Biomedical Products, Bedford, MA) placed between the lower chamber and the upper chamber. Huh7 were suspended in DMEM at a concentration of 10^6/mL, and 1×10^5 cells were added to the upper chamber. The lower chamber was filled with DMEM (200 μL) containing 5% FBS. Migration was evaluated after 12 hours by counting the cells stained with crystal violet that had migrated to the lower surface of the polycarbonate filters by using a Zeiss microscope (Oberkochen, Germany) equipped with bright-field optics. For each filter, the number of cells in six randomly chosen fields was counted and the counts were averaged (mean ± SD). Results are expressed as the number of migrated cells per high power field.

Flow cytometry analysis. Cells were plated on 100 mm Petri dishes and treated with ABT-100 or DMSO 48 hours in DMEM with 10% FBS. Cells were harvested using 3 mL trypsin-EDTA and washed twice with PBS. Cells were resuspended at 1×10^6 mL in a solution containing 25 μg/mL propidium iodide, 0.02% Nonidet P-40, and 0.5 mg RNase A in PBS. Samples were incubated in the dark at room temperature for 30 minutes and stored at 4°C. Cell cycle phases were determined in a FACScan flow cytometer (Becton Dickinson, San Jose, CA). The proportion of apoptotic cells (Apo) corresponding to cells with a DNA content less than 2 N and cells in G_1, S, and G_2-M phase were calculated from the respective DNA histograms using the Cellfit software.

Ras processing and Ras-GTP pull-down assay. Cells were seeded on day 0 in 100 mm dishes; different doses of ABT-100 or vehicle (10 mmol/L DTT in DMSO) on days 1 and 2 were employed. On day 1, cell treatment with ABT-100 was done in DMEM with 10% FBS, whereas on day 2, cells were incubated with ABT-100 in DMEM without serum.

On day 3, cells were stimulated with 10% FBS for 15 minutes where indicated and then washed, harvested, and lysed in buffer containing 50 mmol/L HEPES (pH 7.5), 150 mmol/L NaCl, 1% Triton X-100, 5 mmol/L $MgCl_2$, 1 mmol/L EDTA, 2 mmol/L Na_3VO_4, 10 μg/mL soybean trypsin inhibitor, 20 μg/mL leupeptin, 5 μmol/L pepstatin, and 2 mmol/L phenylmethylsulfonyl fluoride. Lysates were cleared (13,000 rpm, 4°C, 15 minutes), and an equal amount of protein was resolved on a SDS-PAGE 6% to 20% gradient gel, transferred to polyvinylidene fluoride membrane (Millipore Corp., Bedford, MA), and immunoblotted using an anti-pan-Ras mouse monoclonal antibody or an anti-Rap1A polyclonal antibody. Antibody reactions were visualized using peroxidase-conjugated secondary antibodies and an enhanced chemiluminescence detection system (Amersham, Buckinghamshire, United Kingdom).

The Ras-GTP pull-down assay was done employing the pGEX2T-Ras-binding domain construct [encoding a glutathione *S*-transferase (GST) fusion protein containing amino acids 51-131 of c-Raf]. GST-Ras-binding domain expression in *E. coli* was induced with 1 mmol/L isopropyl-L-thio-β-D-galactopyranoside for 2 hours. Bacteria were sonicated in 50 mL PBS containing 0.5 mmol/L DTT and protease inhibitor. After the addition of 1% Triton X-100, clarified lysates were aliquoted and stored at −80°C. The fusion protein was bound to glutathione-Sepharose beads. For affinity precipitation, the cell lysates were incubated with beads for 30 minutes and collected by centrifugation at 13,000 rpm. After washing thrice with lysis buffer and incubation in loading buffer, samples were separated in 15% SDS-PAGE and subjected to immunoblot using a pan-Ras antibody to identify Ras-GTP.

Immunoprecipitations and immunoblotting. After treatment with ABT-100, cells were harvested and nuclear or cytoplasmic proteins were differentially extracted by using ice-cold hypotonic lysis buffer [0.2% NP40, 10 mmol/L HEPES (pH 7.9), 1 mmol/L EDTA, 60 mmol/L KCl]. Nuclei were separated through a 30% sucrose and lysed in hypertonic buffer [250 mmol/L Tris-HCl (pH 7.8), 60 mmol/L KCl].

The extracts were centrifuged for 10 minutes at 13,000 rpm and the supernatant was used for immunoprecipitation or immunoblotting.

For immunoprecipitations, antibodies were added to cell lysates and incubated overnight at 4°C, and antibodies collected on protein A Sepharose beads. Protein complexes were washed in an immunoprecipitation buffer [50 mmol/L Tris-HCl (pH 7.4), 0.5 mol/L NaCl, 1 mmol/L $CaCl_2$, 1 mmol/L $MgCl_2$, 0.1% Tween 20] prior to direct analysis by SDS-PAGE or *in vitro* ^{32}P-labeling. Proteins were resolved by 12% SDS-PAGE and transferred to polyvinylidene difluoride. The membranes were blocked for 1 hour at room temperature in 2% gelatin PBS solution and subsequently probed in the same solution with antibodies (Upstate Biotechnology). The membranes were then washed with PBS/0.1% Triton X-100, and enhanced chemiluminescence was used for detection.

PI3K and Akt kinase assay. To assay PI3K activity, aliquots of cell extracts that contained equivalent amounts of protein were incubated overnight with antiphosphotyrosine antibodies (PY99, Santa Cruz Biotechnology) and protein A Sepharose. The Sepharose beads were washed twice with lysis buffer and twice with 10 mmol/L Hepes buffer containing 0.1 mmol/L EGTA (kinase buffer). After removal of the last wash, the beads were resuspended in kinase buffer containing 20 μg of sonicated L-α-phosphatidylinositol (Sigma) 25 mmol/L $MgCl_2$ and 10 μCi [γ^{32}P]ATP, and incubated for 10 minutes at room temperature. The reaction was stopped by the addition of 60 μL 6 N HCl and 160 μL of a mixture of chloroform and methanol. Lipids were resolved by TLC plates coated with potassium oxalate.

To assay Akt kinase activity, total cell extracts containing equivalent amounts of protein were incubated with a sheep polyclonal antibody that recognizes Akt1/PKBα (Upstate Biotechnology, catalogue #06-558) overnight. After 1-hour incubation with protein A and G Sepharose mixture, the beads were washed thrice with lysis buffer once with water and once with kinase buffer [20 mmol/L Hepes (pH 7.4), containing 10 mmol/L $MgCl_2$ and 10 mmol/L $MnCl_2$]. After removal of the last wash, the beads were resuspended in 30 μL of kinase buffer containing 5 μmol/L ATP, 1 mmol/L DTT, 10 μCi [γ^{32}P]ATP, and 2 μg of histone H2B and incubated for 20 minutes at room temperature. The reaction was stopped by the addition of Laemmli sample buffer and resolved by SDS-PAGE (15%).

CDK2 assay. To measure the activity of CDK2, histone H1 was used as a substrate. CDK2 was immunoprecipitated using a rabbit polyclonal anti-CDK2 (M2, Santa Cruz Biotechnology) in a 30 μL reaction mixture containing 50 mmol/L HEPES (pH 7.4), 10 mmol/L $MgCl_2$, 5 mmol/L $MnCl_2$, 1 mmol/L DTT, 10 μCi [γ^{32}P]ATP, and 100 μg/mL histone H1 which was incubated for 30 minutes at 30°C. The reaction was terminated by the addition of an equal volume of SDS-PAGE sample buffer. The samples were fractionated by SDS-PAGE, the gel was stained, dried and exposed to Kodak X-Omat AR film at −70°C.

RNA interference of p27^{Kip1}. The small interfering RNA (siRNA) sequence targeting human p27^{Kip1} (Genbank accession number AY004255) spans nucleotides 469 to 489 and is specific for p27^{Kip1} based on BLAST search (National Center for Biotechnology Information database). A siRNA sequence corresponding to nucleotides 695 to

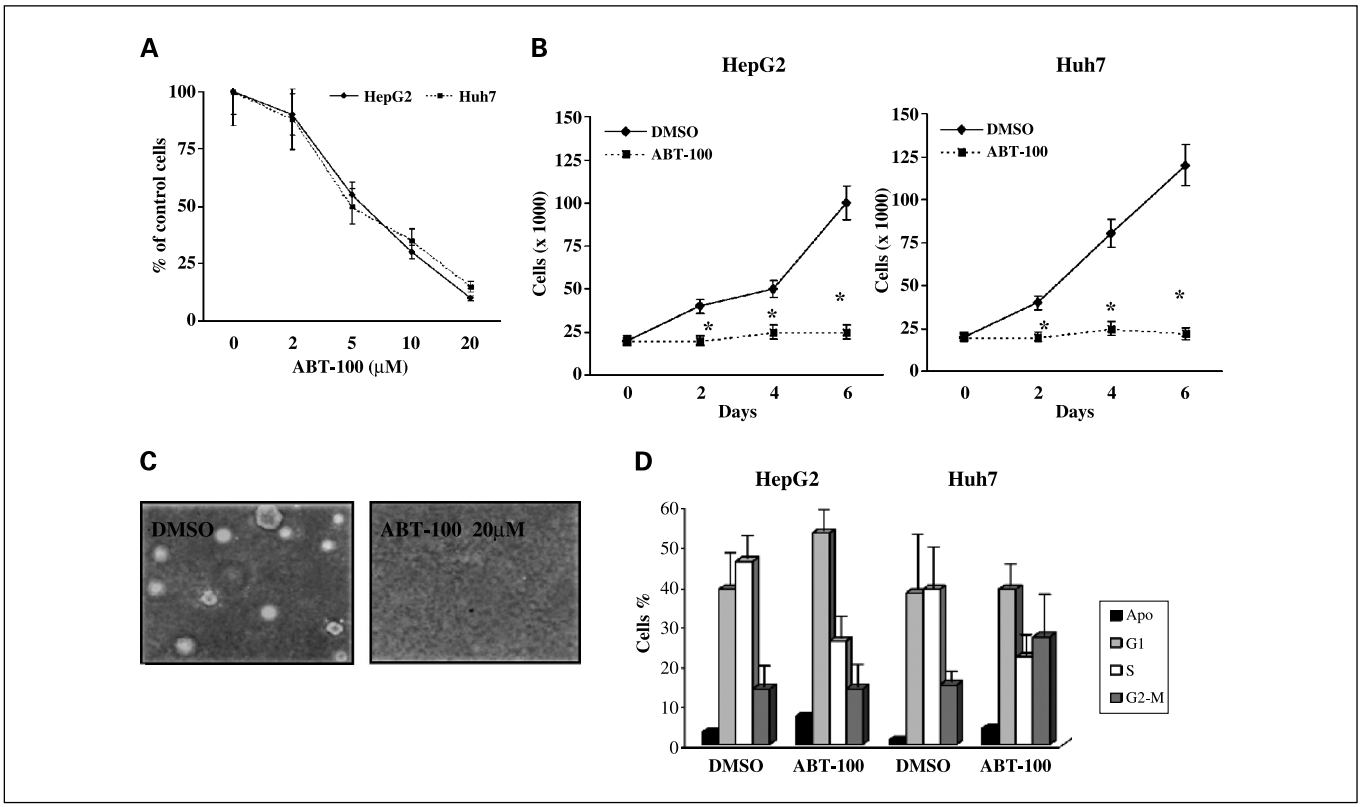

Fig. 1. Inhibition of HepG2 and Huh7 cell proliferation by ABT-100. *A*, cell growth inhibition assay was done by plating 2×10^4 cells on 12-well plates, in DMEM with 10% FBS. Cells were counted after 48 hours' incubation with increasing concentration of ABT-100 in DMEM with 10% FBS. Results are expressed as a percentage of control cells, and each value is the mean of two separate experiments done in triplicate. *B*, cell growth inhibition assay was done by plating 2×10^4 cells on 12-well plates in DMEM with 10% FBS. Cells were treated with ABT-100 (20 μmol/L) or DMSO every 48 hours for 6 days and the number of cells was determined at the time points 2, 4, or 6 days by counting with a hemocytometer. The viability of cells was measured by the trypan blue dye exclusion method. Results are expressed as cells per well and each value is the mean of three separate experiments done in triplicate. *, $P < 0.05$ or higher degree of significance versus controls. *C*, soft agar growth assay. Huh7 cells were seeded into soft agar and treated with DMSO or ABT-100. Cells were photographed 14 days later. *D*, effect of ABT-100 on the cell cycle distribution. HepG2 and Huh7 were seeded and treated for 48 hours with DMSO or ABT-100 (20 μmol/L) in DMEM plus 10% FBS. On day 3, cells were harvested and analyzed by propidium iodide staining and flow cytometry. Apoptotic cell populations (Apo) were evaluated by using Cellfit software (Becton Dickinson Systems). *Columns*, means; *bars*, ± SD.

715 of the firefly luciferase (U31240) was used as negative control. RNA duplexes were synthesized by Qiagen (Germany).

Huh7 cells were plated in 6 cm dishes at 30% confluence for 24 hours and transfected with 10 μL of 20 μmol/L siRNA and 3 μL of OligofectAMINE in 1 mL Opti-MEM. After 5 hours, cells were washed and cultured in DMEM containing FBS.

Experimental hepatocarcinogenesis. Two groups of 13 female Wistar rats (210-225 g) were given diethylnitrosamine 50 mg/L ad libitum in their drinking water for a period of 10 weeks. Another group of six animals were maintained as controls. All animals received a standard laboratory diet and were weighed each week.

On the first day of ABT-100 treatment (10 weeks after diethylnitrosamine administration), the animals were randomized into group 1 (13 rats) to which was given daily ABT-100 (25 mg/kg/day) by s.c. injection for 4 weeks. This dose level of ABT-100 was chosen because it was previously assessed to be effective in human tumor xenograft studies in nude mice. Group 2 (13 rats) received daily injection of ABT-100 vehicle. At the end of the 4th week of treatment with ABT-100, the rats were sacrificed. The livers were harvested and the fresh tumors were sized and counted independently by two investigators.

Statistical analysis. Results are expressed as means ± SD. Statistical analysis of results was done by Student's *t* test, comparing the compound group with the control group.

Results

Effect of ABT-100 on cell growth and invasiveness in liver cancer cells. To evaluate the effects of ABT-100 on cell growth, we used the two liver cancer cell lines, HepG2 and Huh7. Cells were counted after 48 hours of incubation with increasing concentrations of ABT-100 in DMEM with 10% FBS (Fig. 1A) or were treated with ABT-100 (20 μmol/L) and the growth rate was evaluated after 2, 4, and 6 days (Fig. 1B). The growth rate of HepG2 and Huh7 cells treated with ABT-100 was significantly lower in comparison to control cells treated with vehicle alone. These results were further confirmed in a soft agar growth assay (Fig. 1C).

Next, we evaluated the effect of ABT-100 on HepG2 and Huh7 cell cycle distribution. Cells were seeded in DMEM plus 10% FBS and were treated with DMSO or ABT-100 (20 μmol/L) for 48 hours. DNA content was analyzed by flow cytometry after staining with propidium iodide. The results showed that ABT-100 acted prevalently, blocking the entry of cells in S phase of cell cycle. Particularly, HepG2 were arrested in the G_1 phase, whereas Huh7 showed an increased number of cells in the G_2-M phase (Fig. 1D).

We also investigated through flow cytometry whether ABT-100 was able to induce apoptosis. The addition of 20 μmol/L ABT-100 did not lead to the appearance of a significant fraction of cells in the region corresponding to cells with a DNA content less than 2 N, a characteristic aspect of apoptotic cells.

A clinically important aspect of the pathology of hepatocellular carcinoma is the ability of these tumors to invade and metastasize. Therefore, we evaluated the effect of ABT-100 on the invasiveness of Huh7. As shown in Fig. 2A, ABT-100 blocked Huh7 cell invasion of Matrigel in a dose-dependent manner.

Effects of ABT-100 on Ras and Rap1A processing and Ras activation. The ability of ABT-100 to selectively inhibit protein farnesylation of HepG2 and Huh7 cells was tested by treating cells with DMSO (vehicle) or ABT-100 (20 μmol/L). The resulting cell lysates were immunoblotted with antibodies against Ras and Rap1A. As shown in Fig. 2B, the pan-Ras

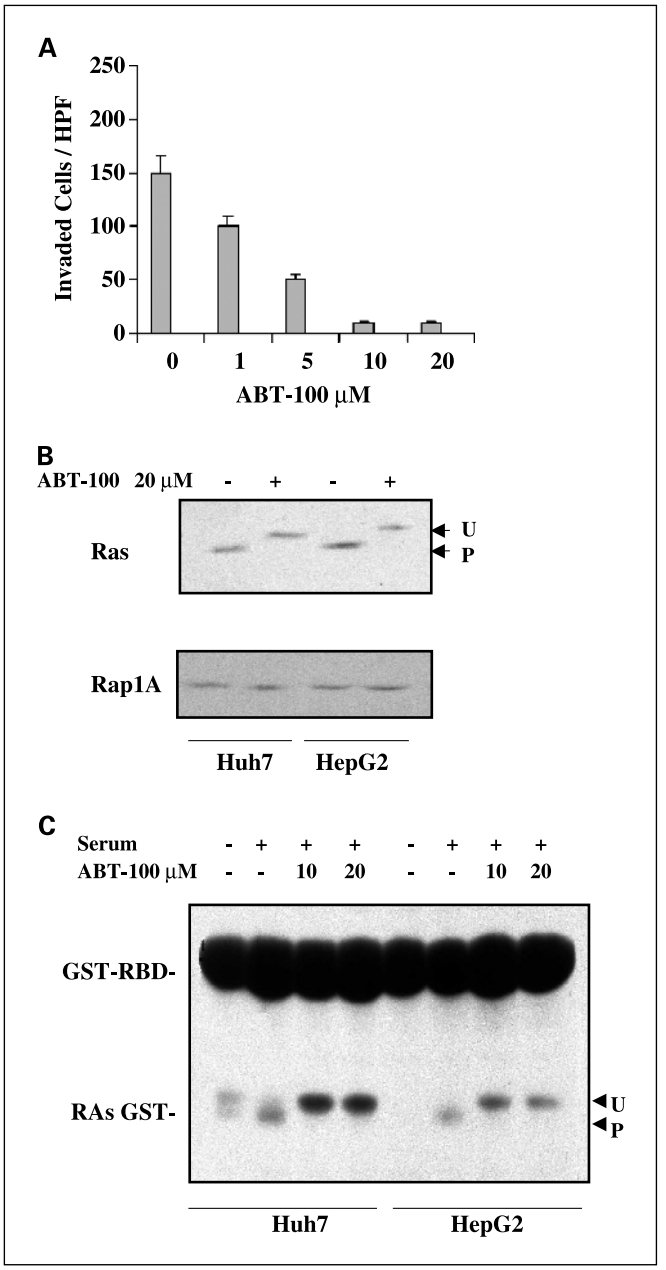

Fig. 2. Effects of ABT-100 on cell invasion and Ras activation. *A*, Huh7 were plated on 100 mm dishes and treated with different doses of ABT-100 or DMSO on days 1 and 2. On day 1, cell treatment with ABT-100 was done in DMEM with 10% FBS, whereas on day 2, cells were incubated with ABT-100 in DMEM without serum. Huh7 were placed in serum-free DMEM in the upper compartment of the Boyden chamber and tested for migration through a filter coated in the upper side with Matrigel. Cells that had migrated to the lower surface of the filter after 12 hours were stained and visually measured by cell counting. The values (number of cells that migrated per high-power field); *columns*, means; *bars*, ± SD, from six separate fields counted in three different experiments. *B*, to show the ability of ABT-100 to selectively inhibit protein farnesylation of HepG2 and Huh7 cells, we treated these cells with DMSO or ABT-100 (20 μmol/L) and the cell lysates were immunoblotted with antibodies against Ras and Rap1A. The pan-Ras antibody detected Ras protein in both cell lines. Treatment of HepG2 and Huh7 with ABT-100 resulted in inhibition of Ras processing as indicated by the shift of Ras band. In contrast, ABT-100 was unable to alter the electrophoretic mobility of Rap1A, a geranylgeranylated protein. *U*, unprocessed; *P*, processed. *C*, to evaluate the effect of ABT-100 on Ras activation we did a pull-down assay. The cells were pretreated with ABT-100, then serum-starved overnight, and finally stimulated with FBS 10% for 15 minutes. The binding of Ras-GTP with GST-Ras-binding domain (of c-Raf) was evaluated as described under Materials and Methods. Data are representative of three independent experiments. *U*, unprocessed; *P*, processed.

antibody detected Ras protein in both cell types. Treatment of HepG2 and Huh7 with ABT-100 resulted in inhibition of Ras processing as indicated by the mobility shift of Ras on SDS-PAGE. In contrast, ABT-100 was unable to alter the electrophoretic mobility of Rap1A, a geranylgeranylated protein. Taken together, these results indicate that ABT-100 is a specific inhibitor of Ras farnesylation and does not interfere with the processing of geranylgeranylated proteins.

To evaluate the effect of ABT-100 on Ras activation, we did a pull-down assay to detect the binding of Ras-GTP with GST-Ras-binding domain. The cells were pretreated for 48 hours with ABT-100 and then were serum-starved overnight, and finally stimulated with FBS 10% for 15 minutes. Figure 2C shows that treatment on with ABT-100, increased levels of unprocessed Ras-GTP were observed in both cell lines.

Treatment of ABT-100 inhibits PI3K/Akt activation. Several lines of evidence have shown that PI3K is required for Ras transformation, therefore, we evaluated the effects of ABT-100 on PI3K activity. HepG2 and Huh7 cells were seeded on day 0 and on day 1 cells were treated with DMSO or ABT-100 in DMEM plus 10% FBS. On day 2, cells were incubated with DMSO or ABT-100 in DMEM without serum. The day after the cells were stimulated for 15 minutes with 10% serum. As shown in Fig. 3A and B, ABT-100 inhibited serum-induced PI3K activity in Huh7 and HepG2. Furthermore, ABT-100 inhibited p85 regulatory subunit tyrosine phosphorylation in Huh7cells. (Fig. 3C).

Given the link between PI3K and Akt/PKB activation we assessed whether the inhibitory activity of PI3K was present on Akt/PKB. ABT-100 resulted in inhibition of serum-induced Akt/PKB Ser473 phosphorylation, and the effect was also observed in an Akt/PKB kinase assay (Fig. 4A and B). Immunocomplex kinase assay was carried out with an anti-Akt/PKB polyclonal antibody, and the immunoprecipitates were subjected to *in vitro* kinase assay using histone H_2B as the substrate.

Because transformation of hepatocytes is often associated with chronic activation of the mitogen-activated protein kinase pathway, we evaluated the effects of ABT-100 on serum-induced MEK1/MEK2 phosphorylation. MEK1 and MEK2 are

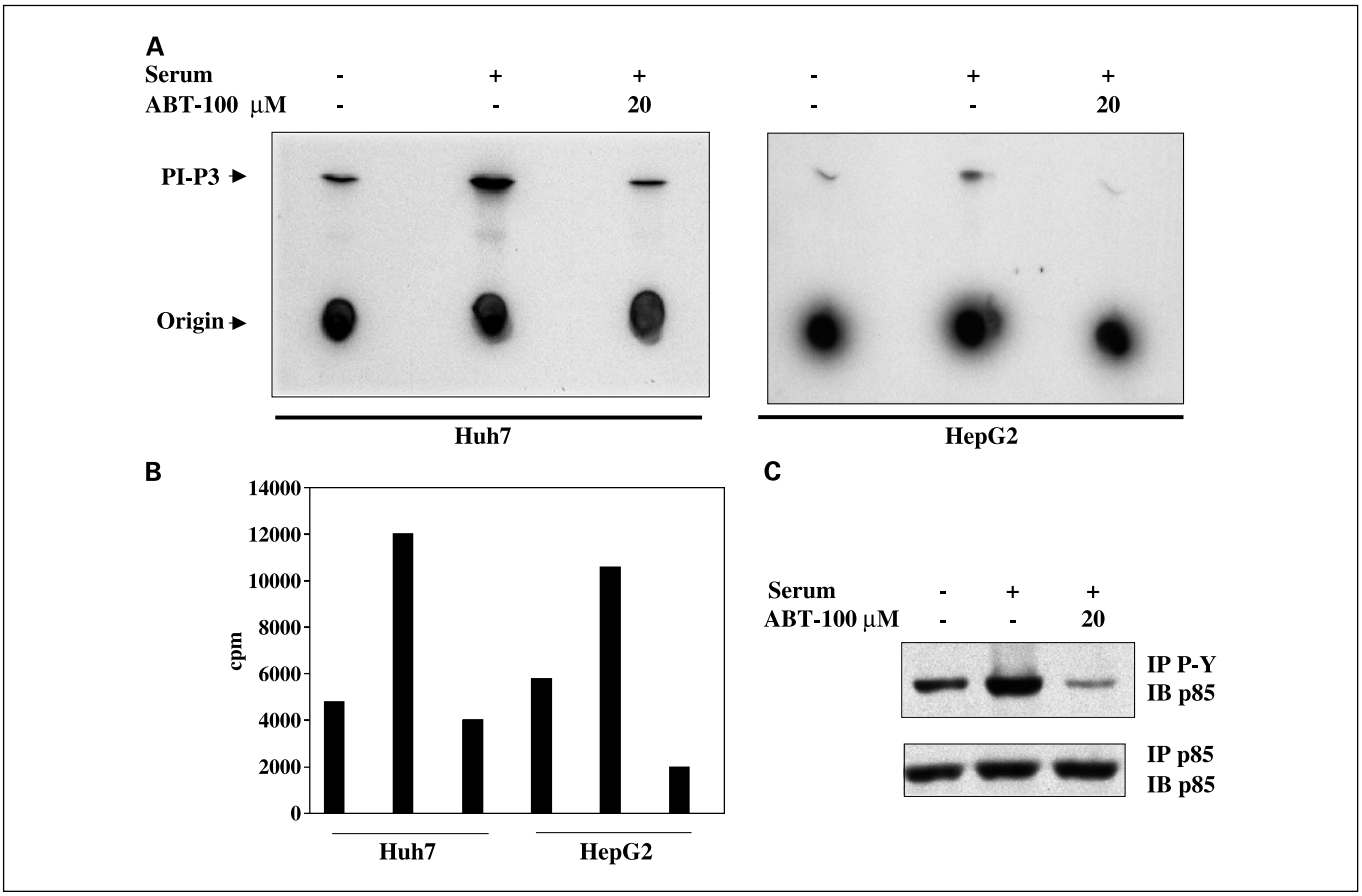

Fig. 3. ABT-100 inhibits PI3K activity and p85 tyrosine phosphorylation. *A*, cells were seeded on day 0 in 100 mm dishes. On day 1, cell treatment with 20 μmol/L ABT-100 was done in DMEM with 10% FBS, whereas on day 2, cells were incubated with ABT-100 in DMEM without serum. On day 3, cells were stimulated with 10% FBS for 15 minutes where indicated and then washed and harvested. Cells were lysed and lysates were immunoprecipitated with anti-P-Tyr monoclonal antibody. Immunoprecipitates were subjected to a kinase assay in the presence of [γ^{32}P]ATP and phosphatidylinositol. Autoradiogram of the kinase reaction after TLC is shown. The position of the 3′ phosphorylated phosphatidylinositol (PI-P3) is indicated. *B*, β-emitting radioactivity corresponding to PI-P3 was quantified using a β-counter. Lipid kinase activity is expressed as cpm within a defined area representing the PI-P3 spot. The result is representative of three independent experiments. *C*, Huh7 cells were seeded on day 0 in 100 mm dishes. On day 1, cell treatment with 20 μmol/L ABT-100 was done in DMEM with 10% FBS, whereas on day 2, cells were incubated with ABT-100 in DMEM without serum. On day 3, cells were stimulated with 10% FBS for 15 minutes where indicated and then washed and harvested. Cells were lysed and lysates were immunoprecipitated with antiphosphotyrosine antibodies. The p85 subunit was revealed by immunoblotting. Data are representative of three independent experiments.

dual-specificity protein kinases that function in activating mitogen-activated protein kinase pathways and controlling cell growth and differentiation. Treatment with ABT-100 did not affect MEK1/MEK2 phosphorylation of HepG2 and Huh7 cells (Fig. 4C).

ABT-100 inhibits Akt/PKB-dependent phosphorylation of $p27^{Kip1}$. The next step was to correlate the inhibiting efficacy of ABT-100 on cell proliferation and PI3K/Akt signaling pathway. First of all, we addressed whether ABT-100 treatment affected the expression of mitotic inhibitors such as $p27^{Kip1}$ in Huh7 cells. ABT-100 treatment of cells increased protein levels of p27Kip1 and the increase was localized to the nuclear fraction of Huh7 (Fig. 5A). Moreover, we evaluated the ability of ABT-100 to influence the activity of the CDK2, a kinase controlled by $p27^{Kip1}$. Huh7 cells were treated with ABT-100 (20 μmol/L) and the resulting lysates were immunoprecipitated with anti-CDK2 antibody. Figure 5B shows that CDK2 from serum-treated Huh7 cells was active and able to phosphorylate histone H1 in an immune complex kinase assay *in vitro*. Prior treatment of cells with ABT-100 blocked CDK2 activity. To find out whether the reduced CDK2 activity was related to $p27^{Kip1}$, we verified the existence of an association between CDK2 and $p27^{Kip1}$. As shown in Fig. 5B (*middle*), $p27^{Kip1}$ was co-immunoprecipitated with CDK2.

Recently, several reports have described the ability of activated Akt to phosphorylate $p27^{Kip1}$, sequestering the protein in the cytoplasmic compartment. Our findings that ABT-100 inhibited Akt activity and increased protein levels of $p27^{Kip1}$ in the nucleus, in comparison to the cytoplasmic fraction, prompted us to investigate whether ABT-100 could suppress the activity of Akt in phosphorylating $p27^{Kip1}$. As shown in Fig. 5C, ABT-100 treatment of Huh7 cells was effective in inhibiting recombinant $p27^{Kip1}$ phosphorylation. To further confirm the role played by $p27^{Kip1}$ as a crucial component of ABT-100 inhibitory effects, we used RNA silencing procedures (16). Immunoblotting of Huh7 cell lysates (Fig. 5D) showed that $p27^{Kip1}$ protein expression was reduced to 86% of control levels at 48 hours after exposure to siRNA and the decrease was specific for $p27^{Kip1}$. Huh7 cells with knockdown $p27^{Kip1}$ protein expression showed a defective susceptibility to ABT-100 treatment as illustrated in Fig. 5E, thus establishing the essential role of $p27^{Kip1}$.

Chemopreventive efficacy studies in a model of hepatocarcinogenesis. The pathophysiology of hepatocellular carcinoma has been investigated in mouse models where liver tumors have been induced by carcinogens. The morphologic characteristics of these chemically induced tumors are very similar to those of human tumors (17). Diethylnitrosamine induces an inflammatory process that, in initiated hepatocytes, determines promotion and progression. Foci of cellular alteration seem as early lesions and, at later stages, more progressed carcinomas have been found, which finally give rise to metastases (18, 19).

We used a model of chemical carcinogenesis in which rats were treated with diethylnitrosamine for 10 weeks. In diethylnitrosamine-treated rats at 10 weeks, there was necroinflammation. In addition, there were altered foci in which the hepatocytes were smaller than normal and with a basophilic cytoplasm. Groups of hepatocytes showing ballooning degeneration were also evident. After 14 weeks, livers showed evidence of hepatocellular carcinoma. Neoplastic changes were seen throughout all livers. Necroinflammation was less marked compared with week 10 animals.

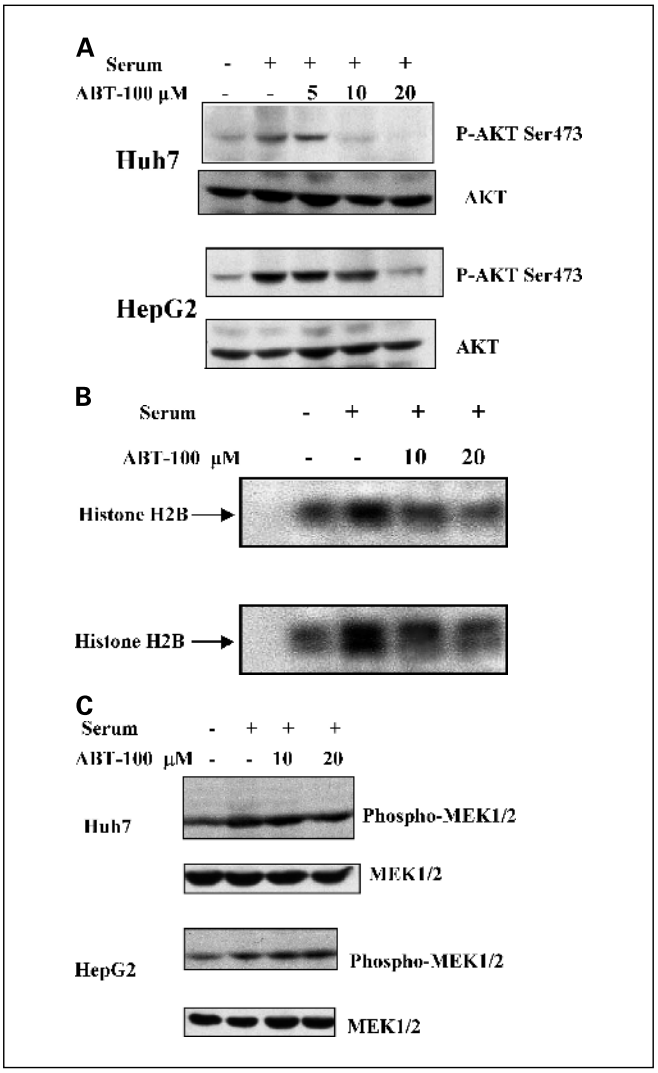

Fig. 4. Effects of ABT-100 on Akt kinase activity and MEK activation. Cells were seeded on day 0 in 100 mm dishes; different doses of ABT-100 or vehicle on days 1 and 2 were employed. On day 1, cell treatment with ABT-100 was done in DMEM with 10% FBS, whereas on day 2, cells were incubated with ABT-100 in DMEM without serum. On day 3, cells were stimulated with 10% FBS for 15 minutes where indicated, and then washed and harvested. Equal amounts of proteins were resolved by 12% SDS-PAGE and immunoblotted anti-P-Akt Ser^{473} (*A*) or anti-P-MEK1/2 (*C*). Equal amounts of proteins were immunoprecipitated with a polyclonal antibody directed against Akt and kinase activity was evaluated as ability to phosphorylate histone H2B, (*B*). Data are representative of three independent experiments.

Based on the natural history of diethylnitrosamine-treated rats, we decided to give ABT-100 for 4 weeks starting at 10 weeks after diethylnitrosamine discontinuation.

ABT-100 had been previously given by the s.c. route to severe combined immunodeficiency (doses up to 12.5 mg/kg/day for 21 days) and nude mice (doses up to 25 mg/kg/day for 21 days). In these experiments, doses as low as 6.25 mg/kg were efficacious when given treatment by the s.c. route (20).

ABT-100 is highly bioavailable and when given to rats at doses up to 150 mg/kg/day for 14 days, no overt signs of toxicity were observed, although decreases in neutrophils and platelets were induced at 50 and 150 mg/kg/day. Based on

plasma drug concentrations achieved in nude mouse efficacy studies, we gave 25 mg/kg/day by s.c. injection. As shown in Table 1, ABT-100 significantly reduced the incidence, multiplicity, and volume of liver tumors.

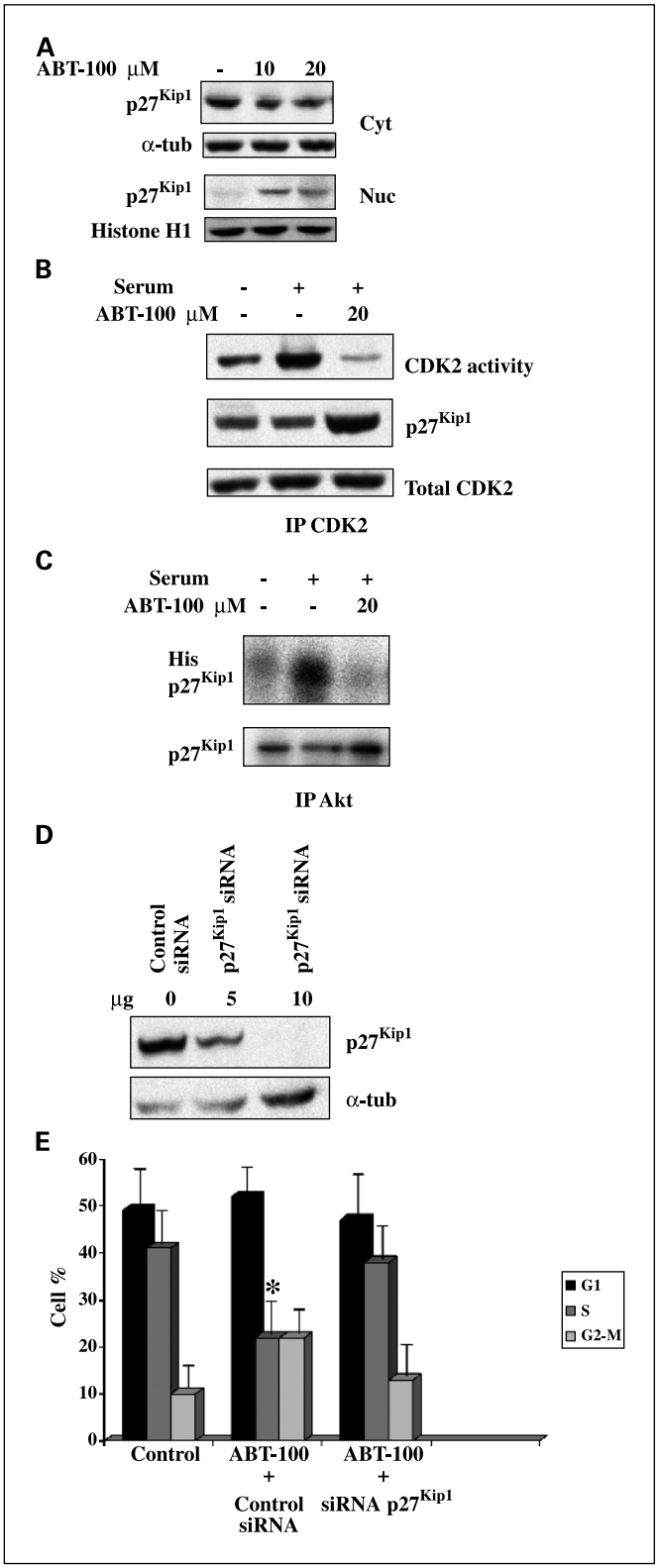

Discussion

In this study we have investigated the effects of the novel farnesyltransferase inhibitor ABT-100 *in vitro* and *in vivo*. ABT-100 is a highly potent (IC_{50} = 0.05 nmol/L) inhibitor of the farnesyltransferase and displays >100,000-fold selectivity relative to geranylgeranyltransferase I. ABT-100 was at least 4-fold more potent than R-115777, SCH-66336, and BMS-214662 in inhibiting the anchorage-independent growth of NIH3T3-H-Ras and human colon carcinoma HCT 116 cells, and its activity was barely affected by human serum or the multidrug resistance phenotype. Inhibition of corneal neovascularization was also observed in a mouse model. Pharmacokinetic studies in mice, dogs, and monkeys showed good oral bioavailability and it seems to have a relatively long half-life. Tumor growth-inhibitory activity was seen following oral and s.c. administration in human lung, colon, and bladder carcinoma xenograft models (20).

Our studies show that ABT-100 is also a potent inhibitor of hepatocarcinogenesis and identify the proteins PI3K, Akt, and $p27^{Kip1}$ as targets of ABT-100 action.

In both cell types, ABT-100 inhibits growth and the entry of cells in the S phase of the cell cycle (21, 22). Our results support the notion that cell cycle arrest is due to increased levels of the CDK inhibitor, $p27^{Kip1}$. $p27^{Kip1}$ levels are highest in quiescent cells and decline as cells reenter the cell cycle. This implies that reduced expression of $p27^{Kip1}$ may predispose cells to abnormal cell cycle and tumor progression (23–26). Hence, increased expression of $p27^{Kip1}$ induced by ABT-100 may provide a protective effect on tumor progression (27). Furthermore, in this report, we provide evidence that ABT-100 inhibits PI3K and Akt kinase activity. Two different mechanisms of activation of PI3K have been described *in vitro*. First, activation can occur by binding of the 85 kDa regulatory subunit of PI3K to tyrosine kinase receptors. Second, activation can occur by binding of constitutively active Ras to the 110 kDa catalytic subunit. *In vivo*, both interactions result in increased phosphoinositide synthesis, and evidence suggests that inhibition of either of the two mechanisms affects PI3K activation (28). Our findings reveal that inhibition with ABT-100 results in the accumulation of nonfarnesylated Ras-GTP in the cytoplasm as previously shown by Lerner et al. (29). However, in this condition, unprocessed Ras-GTP is still able

Fig. 5. ABT-100 inhibits Akt-dependent $p27^{Kip1}$ phosphorylation and restores $p27^{Kip1}$ nuclear effects. *A*, Huh7 cells were seeded in 100 mm dishes; different doses of ABT-100 were employed, and cytosolic and nuclear fractions were separated, then endogenous $p27^{Kip1}$ was immunoblotted. Loading controls were evaluated by blotting against α-tubulin and histone H1, respectively. *B*, CDK2 was immunoprecipitated using a rabbit polyclonal anti-CDK2 antibody and histone H1 was used as substrate in an immunocomplex kinase assay, as described in Materials and Methods. The samples were separated by SDS-PAGE, and visualized by autoradiography (*top*). Immunoprecipitated CDK2 was resolved and immunoblotted against $p27^{Kip1}$ to show association (*middle*). Protein loading was evaluated by immunoblotting against CDK2 (*bottom*). *C*, Huh7 cell lysates were immunoprecipitated with a polyclonal antibody anti P-Akt Ser^{473} and His-Tag $p27^{Kip1}$ was used as substrate in the presence of [γ^{32}P]ATP in an immunocomplex kinase assay. *D*, Huh7 cells were transfected with the indicated concentrations of synthetic siRNA $p27^{Kip1}$ and control siRNA. Forty-eight hours later, cells were lysed and protein extracts were separated and immunoblotted for $p27^{Kip1}$. Loading control was evaluated by blotting against α-tubulin. *E,* after transfection, Huh7 cells were treated 48 hours with 20 μmol/L ABT-100 and then cell cycle analysis was done by flow cytometry. *Columns*, means; *bars*, ± SD. *, $P < 0.05$ or higher degree of significance versus control and Huh7 with knockdown $p27^{Kip1}$.

Table 1. Effects of ABT-100 in diethylnitrosamine-induced hepatocarcinogenesis

Diethylnitrosamine	Treatment	No. rats	Tumor incidence (%)	Tumor multiplicity	Total tumor volume (mm^3)
Group 1	ABT-100	13	42*	10.1 ± 7.3†	2.8 ± 0.4‡
Group 2	Vehicle	13	90	31.8 ± 11.2	8.9 ± 2.1

NOTE: Female Wistar rats were given diethylnitrosamine in drinking water for 10 weeks. After diethylnitrosamine discontinuation, rats were randomized to receive ABT-100 (25 mg/kg/day) or ABT-100 vehicle for 4 weeks by s.c. injection.
*$P < 0.05$ compared with vehicle-treated rats.
†$P < 0.01$ compared with vehicle-treated rats.
‡$P < 0.05$ compared with vehicle-treated rats.

to associate with effector proteins such as Raf kinase, thus farnesylation is not required for Ras to bind to Raf. Furthermore, the fact that nonfarnesylated Ras binds Raf in the cytoplasm gives support to the assumption that unprocessed Ras-GTP is a dominant-negative form of Ras. This is an important aspect of Ras biology, in fact, several farnesyltransferase inhibitors possess efficacy on neoplastic cells expressing wild-type Ras.

These results assume relevancy considering the recent advances on Ras interactions with plasma membrane. The new scenario displays Ras proteins interacting dynamically with specific microdomains of the plasma membrane and intracellular membranes (30). The idea that different Ras isoforms associate dynamically with spatially distinct microdomains (i.e., lipid rafts) of the plasma membrane is an important conceptual advance in Ras signaling. The model that has been proposed predicts that K-Ras is associated predominantly with non–raft plasma membrane, irrespective of its activation state. H-Ras is distributed equally between raft and non–raft plasma membrane, but GTP loading increases the fraction of H-Ras in non–raft membrane. GTP loading therefore regulates the lateral segregation of H-Ras in the plasma membrane (31).

These microdomains need to be characterized further, in terms of their composition and function, to verify the underlying hypothesis that the precise microenvironment in which Ras isoforms engage a set of effector proteins governs the ultimate signal output.

It has been described that growth factor–activation of Ras (or constitutively active Ras) can reduce $p27^{Kip1}$ levels by decreasing its translation and stability (32, 33). The present results indicate that Ras farnesylation, PI3K, and Akt regulate $p27^{Kip1}$ cellular expression (34, 35). Progression through the cell cycle is governed by the cyclin-dependent kinases. In mammalian cells, CDK2 is a member of the CDK family and exhibits histone H1 kinase activity that oscillates during the cell cycle. CDK2 activity shows a complex pattern of activation which includes peaks coinciding with the S and G_2 phases of cell cycle (36–38). The results provided in this study suggest that the ability of ABT-100 to arrest liver cancer cell growth is related to the inhibition of CDK2 by nuclear $p27^{Kip1}$ (39–41).

In summary, the present study shows the efficacy of ABT-100 as a prevention drug in a model of hepatocarcinogenesis. The effects obtained imply that most or all of the effects of ABT-100 occur during the promotion/progression phase of tumor development. In particular, the decreased tumor multiplicity that we observe in ABT-100-treated rats are consistent with the primary effects on progression of liver tumors. Although farnesyltransferase inhibitors clearly inhibit Ras farnesylation, it is unclear whether the antiproliferative effects of these compounds are mediated exclusively through their effects on Ras. This study and future studies directed towards determining the pathways inhibited by farnesyltransferase inhibitors during cancer cell growth may lead to the identification of new molecular targets for the next generation of mechanism-based anticancer drugs.

References

1. Llovet MJ, Burroughs A, Bruix J. Hepatocellular carcinoma. Lancet 2003;362:1907–17.
2. Carloni V, Mazzocca A, Ravichandran SK. Tetraspanin CD81 is linked to ERK/MAP kinase signaling by Shc in liver tumor cells. Oncogene 2004;23:1566–74.
3. Carloni V, Mazzocca A, Pantaleo P, Cordella C, Laffi G, Gentilini P. The integrin $\alpha6\beta1$ is necessary for the matrix-dependent activation of FAK and MAPkinase and the migration of human hepatocellular carcinoma cells. Hepatology 2001;34:42–9.
4. Carloni V, Romanelli RG, Mercurio AM, et al. Knockout of $\alpha6\beta1$ integrin expression reverses the transformed phenotype of hepatocellular carcinoma cells. Gastroenterology 1998;115:433–42.
5. Hong WK, Sporn MB. Recent advance in chemoprevention of cancer. Science 1997;278:1073–7.
6. Adjei AA. Blocking oncogenic Ras signaling for cancer therapy. J Natl Cancer Inst 2001;93:1062–74.
7. Mazzocca A, Giusti S, Hamilton DA, Sebti MS, Pantaleo P, Carloni V. Growth inhibition by the farnesyltransferase inhibitor FTI-277 involves Bcl-2 expression and defective association with Raf-1 in liver cancer cell lines. Mol Pharmacol 2003;63:159–66.
8. Gunning TW, Kramer MP, Lubet AR, et al. Chemoprevention of Benzopyrene-induced lung tumors in mice by the farnesyltransferase inhibitor R115777. Clin Cancer Res 2003;9:1927–30.
9. Zhang Z, Wang Y, Lantry EL, et al. Farnesyltransferase inhibitors are potent lung cancer chemopreventive agents in A/J mice with a dominant-negative p53 and/or heterozygous deletion of Ink4a/Arf. Oncogene 2003;22:6257–65.
10. Mangues R, Corral T, Kohl NE, et al. Antitumor effect of a farnesyl protein transferase inhibitor in mammary and lymphoid tumors overexpressing N-Ras in transgenic mice. Cancer Res 1998;58:1253–9.
11. Du Wei, Liu A, Prendergast GC. Activation of the PI-3K-AKT pathway masks the proapoptotic effects of farnesyltransferase inhibitors. Cancer Res 1999;59:4208–12.
12. Testa JR, Bellacosa A. AKT plays a central role in tumorigenesis. Proc Natl Acad Sci U S A 2001;98:10983–5.
13. Aktas H, Cai H, Cooper GM. Ras links growth factor signaling to the cell cycle machinery via regulation of cyclin D1 and the Cdk inhibitor $p27^{KIP1}$. Mol Cell Biol 1997;17:3850–7.
14. Medema RH, Kops GJ, Bos JL, Burgering BM. AFX-like forkhead transcription factors mediate cell-cycle regulation by Ras and PKB through $p27^{Kip1}$. Nature 2000;404:782–7.
15. Viglietto G, Motti LM, Bruni P, et al. Cytoplasmic relocalization and inhibition of the cyclin-dependent kinase inhibitor $p27^{Kip1}$ by PKB/Akt-mediated phosphorylation in breast cancer. Nat Med 2002;8:1136–44.
16. Elbashir SM, Harborth J, Lendeckel W, Yalcin A, Weber K, Tuschl T. Duplexes of 21-nucleotide RNAs mediate RNA interference in cultured mammalian cells. Nature 2001;411:494–8.
17. Graveel RC, Jatkoe T, Madore JS, Holt LA, Farnham JP. Expression profiling and identification of novel genes in hepatocellular carcinoma. Oncogene 2001;20:2704–12.
18. Burr WA, Hillan JK, McLaughlin KE, et al. Hepatocyte growth factor levels in liver and serum increase

during chemical hepatocarcinogenesis. Hepatology 1996;24:1282–7.

19. Pitot HC. Altered hepatic foci: their role in murine hepatocarcinogenesis. Annu Rev Pharmacol Toxicol 1990;30:465–500.

20. Ferguson D, Rodriguez LE, Palma JP, et al. Antitumor activity of orally bioavailable farnesyltransferase inhibitor, ABT-100, is mediated by anti-proliferative, pro-apoptotic and anti-angiogenic effects in xenograft models. Clin Cancer Res 2005;11:3045–54.

21. Oren M. Regulation of the p53 tumor suppressor protein. J Biol Chem 1999;274:36031–4.

22. El-Deiry WS, Tokino T, Velculescu VE, et al. WAF1, a potential mediator of p53 tumor suppression. Cell 1993;75:817–25.

23. Lloyd RV, Erickson AL, Jin L, et al. p27KIP1 a multifunctional cyclin-dependent kinase inhibitor with prognostic significance in human cancers. Am J Pathol 1999;154:313–23.

24. Fero ML, Randel E, Gurley KE, Roberts JM, Kemp CJ. The murine gene $p27^{KIP1}$ is haplo-insufficient for tumour suppression. Nature 1998;396:177–80.

25. Tannapfel A, Grund D, Katalinic A, et al. Decreased expression of p27 protein is associated with advanced tumor stage in hepatocellular carcinoma. Int J Cancer 2000;89:350–5.

26. Singh SP, Lipman J, Goldman H, et al. Loss or altered subcellular localization of p27 in Barrett's associated adenocarcinoma. Cancer Res 1998;58:1730–5.

27. Fiorentino M, Altimari A, D'Errico A, et al. Acquired expression of p27 is a favorable prognostic indicator in patients with hepatocellular carcinoma. Clin Cancer Res 2000;6:3966–72.

28. van Weering JHD, de Rooij J, Marte B, Downward J, Bos LJ, Burgering MTB. Protein kinase B activation and lamellipodium formation are independent phosphoinositide 3-kinase mediated events differentially regulated by endogenous Ras. Mol Cell Biol 1998;18:1802–11.

29. Lerner EC, Qian Y, Blaskovich MA, et al. Ras CAAX peptidomimetic FTI-277 selectively blocks oncogenic Ras signalling by inducing cytoplasmic accumulation of inactive Ras-Raf complexes. J Biol Chem 1995;270:26802–6.

30. Hancock FJ. Ras proteins: different signals from different locations. Nat Rev Mol Cell Biol 2003;4:373–84.

31. Prior IA, Hancock JF. Compartmentalization of Ras proteins. J Cell Sci 2001;114:1603–8.

32. Takuwa N, Takuwa Y. Ras activity late in G_1 phase required for $p27^{KIP1}$ downregulation, passage through the restriction point, and entry into S phase in growth factor-stimulated NIH3T3 fibroblasts. Mol Cell Biol 1997;17:5348–58.

33. Ophaschroensuk V, Fero ML, Hughes J, Shankland SJ. The cyclin-dependent kinase inhibitor $p27^{KIP1}$ safeguards against inflammatory injury. Nat Med 1998;4:575–80.

34. Collado M, Medema HR, Garcia-Cao I, et al. Inhibition of the phosphoinositide 3-kinase pathway induces a senescence-like arrest mediated by $p27^{Kip1}$. J Biol Chem 2000;275:21960–8.

35. Brazil PD, Yang Z-Z, Hemmings AB. Advances in protein kinase B signalling: AKTion on multiple fronts. Trends Biochem Sci 2004;29:233–42.

36. Rosenblatt J, Gu, Y, Morgan DO. Human cyclin-dependent kinase 2 is activated during the S and G_2 phases of the cell cycle and associates with cyclin A. Proc Natl Acad Sci U S A 1992;89:2824–8.

37. Guadagno TM, Newport JW. CDK2 kinase is required for entry into mitosis as positive regulator of Cdc2-cyclin B kinase activity. Cell 1996;84:73–82.

38. Hu Bing Mitra J, van den Heuvel S, Enders HG. S and G_2 phase roles for CDK2 revealed by inducible expression of a dominant-negative mutant in human cells. Mol Cell Biol 2001;21:2755–66.

39. Kato JY, Matsuoka M, Polyak K, Massaguè J, Sherr CJ. Cyclic AMP-induced G_1 phase arrest mediated by an inhibitor $p27^{KIP1}$of cyclin-dependent kinase 4 activation. Cell 1994;79:487–96.

40. Zeng Y, Hirano Khirano M, Nishimura J, Kanaide H. Minimal requirements for the nuclear localization of $p27^{Kip1}$, a cyclin-dependent kinase inhibitor. Biochem Biophys Res Commun 2000;274:37–42.

41. Ciarallo S, Subramaniam V, Hung W, et al. Altered $p27^{Kip1}$ phosphorylation, localization, and function in human epithelial cells resistant to transforming growth factor β-mediated G_1 arrest. Mol Cell Biol 2002;22:2993–3002.

Clinical Cancer Research

Farnesyltransferase Inhibitor, ABT-100, Is a Potent Liver Cancer Chemopreventive Agent

Vinicio Carloni, Francesco Vizzutti and Pietro Pantaleo

Clin Cancer Res 2005;11:4266-4274.